

J. LEE<sup>1\*</sup>, J. JEONG<sup>1</sup>, J. JUNG<sup>1,2</sup>, H. JEONG<sup>1</sup>

# PHASE TRANSITION ENTHALPY, AND OXIDATION BINDING ENERGY OF HYDROTHERMALLY SYNTHESIZED BaTiO<sub>3</sub> NANOPOWDERS VIA PRE-ANNEALING AND SINTERING PROCESSES

Hydrothermally synthesized BaTiO<sub>3</sub> nanopowders pre-annealed at high temperatures of 900°C for 4 h in the air were sintered at 1200°C for 2 h in N<sub>2</sub> atmosphere, and their cubic-tetragonal transformation, transition enthalpy, and binding energy (BE) were investigated. The nanopowder crystal structures changed from cubic to tetragonal during annealing or sintering at temperatures above 900°C with constant tetragonality (1.01). With increasing pre-annealing temperature, the cubic-tetragonal transition enthalpy decreased, and the differential scanning calorimetry (DSC) peak broadened. Pre-annealing in the air increased BE and nonchemical energy distribution in the BaTiO<sub>3</sub> powder, reducing the transition enthalpy and sharpness of the DSC curve. This was ascribed to the differences in imperfections from oxidation, such as the density and uniform distribution of Ba among the samples, resulting from the BE shifts of the Ba 3d, Ti 2p and O 1s peaks to higher values in the XPS spectra.

*Keywords:* Annealing; Sintering; XRD; XPS; DSC

## 1. Introduction

Recently, BaTiO<sub>3</sub> nanopowders have been used as dielectric materials in multilayer ceramic capacitors (MLCCs) owing to their high dielectric permittivities [1,2]. Studies on the high crystallinity and purity of BaTiO<sub>3</sub> nanopowders represent a growing field with the trend toward minimization and improved properties of electronic devices [3]. During the conventional synthesis of BaTiO<sub>3</sub>, solid mixtures of BaCO<sub>3</sub> and TiO<sub>2</sub> are calcinated at a high temperature of approximately 1200°C [4]. In contrast, the hydrothermal synthesis of BaTiO<sub>3</sub> from Ba(OH)<sub>2</sub> and, TiO<sub>2</sub> mixtures can be accomplished at reaction temperatures of 80-150°C and produces finer particles with high purity due to the lower processing temperature. The hydrothermally synthesized BaTiO<sub>3</sub> is often reported to exhibit lower crystallinity and tetragonality, which are related to its polarization and dielectric constant [5].

The factors that influence the crystallinity and tetragonality of hydrothermally synthesized BaTiO<sub>3</sub> powders have been explored in several studies. The Ti precursor, Ba/Ti ratio and synthesis temperature have been considered to be key factors affecting the synthesis time [6,7]. By simply increasing the heating temperature during the annealing process, the BaTiO<sub>3</sub> powder can be transformed from a cubic to a tetragonal structure, with

the increasing tetragonality resulting from the removal of OH groups in the BaTiO<sub>3</sub> powder [8,9]. However, little information is available on the surface electronic states of the Ba, Ti, and O ions, which affect electronic defects and surface reactivity. The surface electronic states can also affect the chemical reactions at the interface of the Ni or Cu electronic layers in MLCCs.

The present study aims to determine the dependence of the tetragonality, transition enthalpy, and electronic states on the binding energies (BEs) of the Ba, Ti, and O ions during the pre-annealing and sintering processes in hydrothermally synthesized BaTiO<sub>3</sub> nanopowders. The correlation between the transition enthalpy and the electronic states of the ions is discussed.

## 2. Experimental Details

The hydrothermally synthesized BaTiO<sub>3</sub> nanopowders with a mean particle size of approximately 100 nm, purity of 99.95% (Shandong Sinocera Functional Material Co., Ltd., China), and cubic structure were prepared before and after annealing at 700 and 900°C for 4 h in air. The pre-annealed nanopowders were compressed into a cylindrical shape with a diameter of 6 mm at a pressure reaching 100 MPa at room temperature, and then,

<sup>1</sup> MATERIALS SUPPLY CHAIN R&D DEPARTMENT, KOREA INSTITUTE OF INDUSTRIAL TECHNOLOGY, INCHEON CITY, 21999, REPUBLIC OF KOREA

<sup>2</sup> INHA UNIVERSITY, DEPARTMENT OF ADVANCED MATERIALS SCIENCE AND ENGINEERING, INCHEON CITY, 22212, REPUBLIC OF KOREA

\* Corresponding author: [ljb01@kitech.re.kr](mailto:ljb01@kitech.re.kr)



the samples were sintered at 1200°C for 2 h in a N<sub>2</sub> atmosphere. The crystal structures of the pre-annealed powder and sintered samples were determined by X-ray diffraction (XRD) using a Rigaku SmartLab instrument. Transition enthalpy determination was carried out using a DSC Q100 (TA Instruments, USA), and samples were studied using the continuous scan mode at a heating rate of 10°C/min under a flowing Ar atmosphere. The surface chemical bonds of the specimens were determined by X-ray photoelectron spectroscopy (XPS, ESCALAB 250Xi, Thermo Fisher Scientific Inc., USA) at room temperature with a base pressure of  $5 \times 10^{-10}$  mbar using monochromatic Al K- $\alpha$  radiation (1486.76 eV) operated at 300 W as the excitation source.

### 3. Results and discussion

X-ray diffraction patterns of the pre-annealed and sintered samples are shown in Fig. 1, and exhibit the characteristic peaks of both the cubic and tetragonal structures of BaTiO<sub>3</sub> without the presence of impurities. For annealing below 900°C (samples 1-2), the BaTiO<sub>3</sub> powders had a cubic structure with signals in the  $2\theta$  range of 44-46°, whereas for annealing or sintering above 900°C (samples 3-6), the profiles of the tetragonal 002 and 200 reflec-

tions appeared in the same range. Based on the XRD patterns obtained using the software for the powerful Rietveld refinement method (Crystal Impact GbR, Germany), the tetragonality ( $c/a$ ) calculated using the lattice parameters of the  $a$  and  $c$  axes reached approximately 1.01 for samples 3-6 (refer to the dashed lines in Fig. 1), thereby indicating that the tetragonality of the BaTiO<sub>3</sub> samples is independent of the sintering temperature and atmosphere after cubic-tetragonal structural transformation occurred. According to previous reports, in hydrothermally synthesized BaTiO<sub>3</sub>, the OH group content in the cubic structure was more stable than that in the tetragonal structure, and the removal of the OH groups by annealing above 800°C increased the tetragonality in the BaTiO<sub>3</sub> [8,9]. Therefore, in the case of samples 4-5, the structural transition in both samples could be due to the high sintering temperature of 1200°C.

Fig. 2 shows the DSC curves of pre-annealed powders and sintered samples, and the protruding area for the heat flow lines of sample 3 in Fig. 2(a) is observed in the range of 120-140°C, indicating the cubic-tetragonal structural transition enthalpy  $\Delta H^{t \rightarrow c}$ . This may be related to the oxygen vacancies, which indicate the defect concentration in the BaTiO<sub>3</sub> structure. In [7], it decreased with increasing defect concentration when using Ba- and Ti-rich samples to induce oxygen vacancies. In this study,

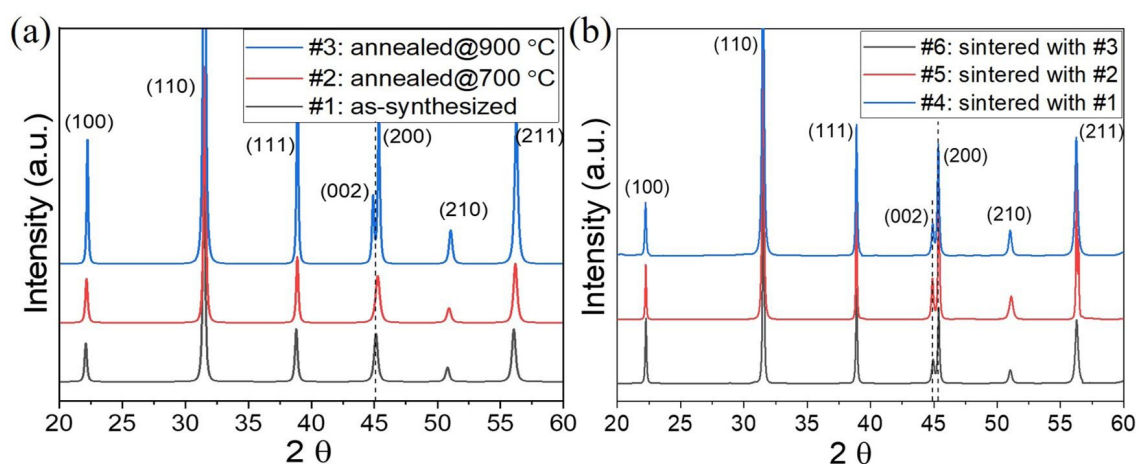


Fig. 1. XRD patterns of (a) pre-annealed powders and (b) sintered samples of the corresponding powders

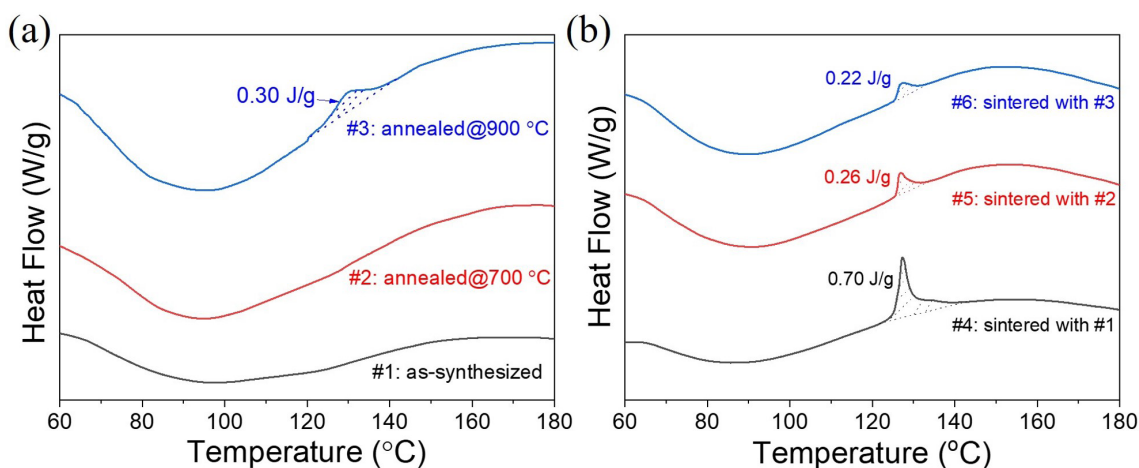


Fig. 2. DSC curves of (a) pre-annealed powders and (b) sintered samples with the corresponding powders

the samples were prepared by annealing at different temperatures in the air; the samples could have various intensities of oxygen absorption, and the defect concentration decreased with annealing temperature. Similar to that reported in [7], the enthalpy changes of the phase transition increased with the annealing temperature in air, owing to the strengthening of the oxidation. As shown in Fig. 2(b), the transition enthalpy of the sintered samples decreased with increasing pre-annealing temperature in air. Although, the crystals of samples 3-6 had a tetragonal structure and the same tetragonality, as shown in Fig. 1, the value of  $\Delta H$  varied with the pre-annealing temperature. Asiaie et al. [10] found that the decrease of the transition enthalpy value was related to the loss of OH in hydrothermally synthesized  $\text{BaTiO}_3$  particles, and the OH group content was reduced by heating below  $800^\circ\text{C}$ . Previous studies also attributed the Ba/Ti ratio [7] and impurities [11] to the transition enthalpy; however, the transition enthalpy variation in this study cannot be related to OH group loss due to the performance of sintering at  $1200^\circ\text{C}$  and other factors mentioned above. In addition, the DSC curve of sample 4 shows sharp peaks, whereas broad peaks are clearly observed for samples 5-6. This broadening with increasing pre-annealing temperature could be caused by the increase in the distribution of nonchemical energy, such as interface, surface, and strain energies, accompanying tetragonal-cubic nucleation/growth. The  $\Delta H$  reduction and peak broadening could improve the densification and uniform distribution for Ba oxidation [12].

Fig. 3 shows the XPS profiles of the pre-annealed and sintered  $\text{BaTiO}_3$  samples in the Ba 3d, Ti 2p, and O 1s regions. The Ba  $3d_{5/2}$  spectrum can be further resolved into three different contributions ( $\text{BaO}_2$ ,  $\text{O}_2/\text{Ba}$ , and  $\text{BaO}$ ), and the BaO peak at the lowest BE of  $778.2\text{ eV}$  in samples 1-5 shifted to  $778.4\text{ eV}$  in sample 6. A second peak attributed to  $\text{BaO}_2$  was observed at a  $1.4\text{ eV}$  higher BE than that of the main BaO peak in the samples of  $\text{BaTiO}_3$  annealed in an oxidizing atmosphere [13]. The lowest BaO peak intensity for sample 1 indicates that oxygen was not cleaved. The spectral line shape of the Ti 2p transitions is shown in Fig. 3(b). The Ti 2p spectrum was deconvoluted into a characteristic spin-orbit split doublet. A chemical shift of

the Ti 2p (Ti  $2p_{3/2}$ , Ti  $2p_{1/2}$ ) level BE toward higher values with increasing pre-annealing temperature was observed, similar to that of Ba  $3d_{5/2}$ . The main peak of Ti  $2p_{3/2}$  is due to the  $\text{Ti}^{4+}$  valence state, and the presence of a shoulder on the lower BE side of the peak demonstrates the existence of  $\text{Ti}^{3+}$  and  $\text{Ti}^{2+}$ , thereby indicating the existence of oxygen vacancies [R8]. The absence of a shoulder in Fig. 3(b) is consistent with the absence of oxygen vacancies near the surface of the entire sample. Fig. 3(c) shows the O 1s spectrum; the lower BE peak at  $528.9\text{ eV}$  belongs to the oxide peak, whereas the higher BE peak can be related to the surface layer termination of the oxides as part of the oxide structure [14]. The shift of the O 1s line to higher values, as indicated by the dashed lines in Fig. 3(c), is comparable those of the Ba 3d and Ti 2p lines. The BE of the main peak ( $528.9\text{ eV}$ ) increases with increasing pre-annealing temperature, which is believed to be due to an increase in the ionic state of the oxygen bond, causing the BEs of all electronic states of oxygen to shift to higher values, which is reported to contribute to the polarization and lattice energy [15]. These positive BE shifts are caused by the oxidation of Ba present with a high density and uniform distribution [16].

#### 4. Conclusions

For the cubic-tetragonal transformation of hydrothermally synthesized  $\text{BaTiO}_3$  nanopowders, the XRD patterns, transition enthalpies, and BEs of chemical reactions via pre-annealing in air and sintering in a  $\text{N}_2$  atmosphere were investigated in this study. The starting powders with a cubic structure were transformed into powders with a tetragonal structure ( $c/a = 1.01$ ) by heating above  $900^\circ\text{C}$ , irrespective of the environment. The transition enthalpy,  $\Delta H^{t \rightarrow c}$ , decreased and the DSC peak broadened with increasing pre-annealing temperature of the sintered samples, which was ascribed to differences in imperfections from oxidation, such as the density and uniform distribution of Ba among samples resulting from the BE shifts of the Ba 3d, Ti 2p and O 1s peaks to higher values in the XPS spectra.

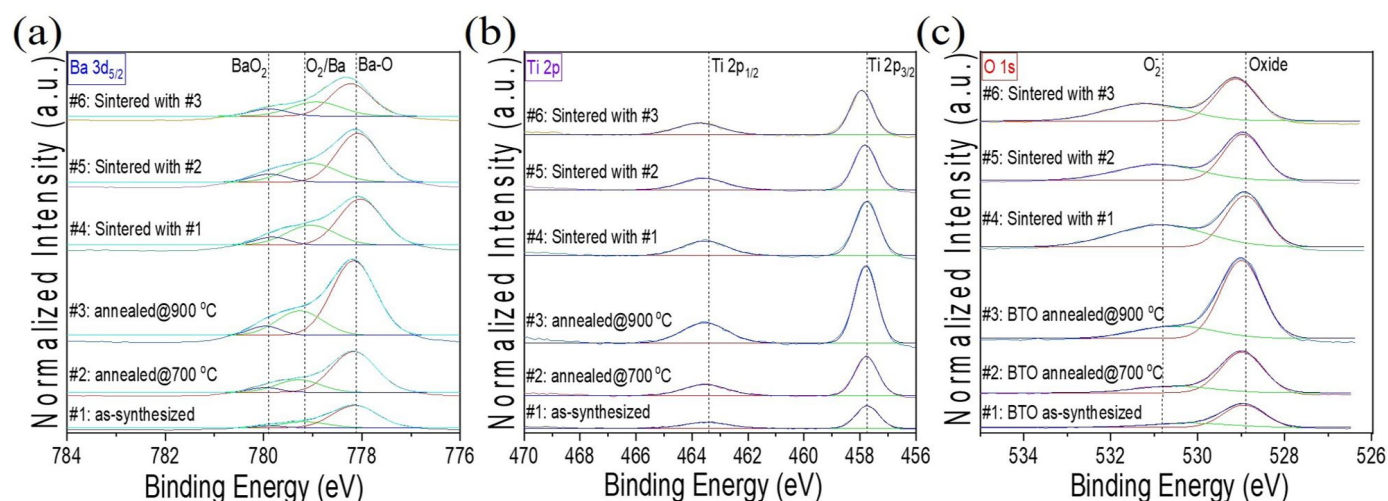


Fig. 3. Decomposition of XPS spectra of the Ba 3d (a), Ti 2p (b), and O 1s regions of pre-annealed and sintered  $\text{BaTiO}_3$  samples

### Acknowledgements

This study was supported by materials & components technology development program funded by the Ministry of Trade, Industry and Energy (MOTIE) (No. 20016519, Development of Ultra-Wide Band communication MLCC for UWB and 5G).

### References

- [1] P.K. Dutta, R. Asiaie, S.A. Akbar, W. Zhu, *Chem. Mater.* **6**, 1545-1546 (1994). DOI: <https://doi.org/10.1021/cm00045a011>
- [2] H. Hayashi, T. Ebina, *J. Ceram. Soc. JAPAN.* **126**, 214-220 (2018). DOI: <https://doi.org/10.2109/jcersj2.17125>
- [3] X. Wei, G. Xu, Z. Ren, G. Shen, G. Han, *J. Am. Ceram. Soc.* **91**, 3774-3780 (2008). DOI: <https://doi.org/10.1111/j.1551-2916.2008.02695.x>
- [4] A. Beauger, J.C. Mutin, J.C. Niepce, *J. Mater. Sci.* **18**, 3041-3046 (1983). DOI: <https://doi.org/10.1007/BF00700786>
- [5] T. Kubo, M. Hogiri, H. Kagata, A. Nakahira, *J. Am. Ceram. Soc.* **92**, S172-176 (2009). DOI: <https://doi.org/10.1111/j.1551-2916.2008.02739.x>
- [6] H. Chen, Y.W. Chen, *Ind. Eng. Chem. Res.* **42**, 473-483 (2003). DOI: <https://doi.org/10.1021/ie010796q>
- [7] S. Lee, *J. Appl. Phys.* **101**, 054119 (2007). DOI: <https://doi.org/10.1063/1.2710280>
- [8] J. Lee, H. Jeong, S. Ma, *Mater. Res. Express* **9**, 065001 (2022). DOI: <https://doi.org/10.1088/2053-1591/ac73e2>
- [9] K. Hongo, S. Kurata, A. Jomphoak, M. Inada, K. Hayashi, R. Maezono, *Inorg. Chem.* **57**, 5413-5419 (2018). DOI: <https://doi.org/10.1021/acs.inorgchem.8b00381>
- [10] R. Asiaie, W. Zhu, S.A. Akbar, P.K. Dutta, *Chem. Mater.* **8**, 226-234 (1996). DOI: <https://doi.org/10.1021/cm950327c>
- [11] F.D. Morrison, D.C. Sinclair, A.R. West, *J. Appl. Phys.* **86**, 6355 (1999). DOI: <https://doi.org/10.1063/1.371698>
- [12] M. Yashima, T. Noma, N. Ishizawa, M. Yoshimura, *J. Am. Ceram. Soc.* **12**, 3011-3016 (1991). DOI: <https://doi.org/10.1111/j.1151-2916.1991.tb04294.x>
- [13] S.M. Mukhopadhyay, T.C.S. Chen, *J. Mater. Res.* **10**, 1502-1507 (1995). DOI: <https://doi.org/10.1557/jmr.1995.1502>
- [14] S. . Nasser, *Appl. Surf. Sci.* **157**, 14-22 (2000). DOI: [https://doi.org/10.1016/S0169-4332\(99\)00495-X](https://doi.org/10.1016/S0169-4332(99)00495-X)
- [15] C.S. Fadley, S.B.M. Hagstrom, M.P. Klein, D.A. Shirley, *J. Chem. Phys.* **48**, 3779 (1968). DOI: <https://doi.org/10.1063/1.1669685>
- [16] D.M. Hill, H.M. Meyer III, J.H. Weaver, *Surf. Sci.* **225**, 63-71 (1990). DOI: [https://doi.org/10.1016/0039-6028\(90\)90424-7](https://doi.org/10.1016/0039-6028(90)90424-7)